Supporting Information

A Gas-Templated CeO_2 Nanoparticle Coating with Tailored Defects for Enhanced UV Durability of PET Films

Liang Zhu [a, *], Yulei Liu [a], Jianyong Huang [a], Liangbin Li [b, *], Changfeng Liu [a], Haichao Qi [a], Jingbin Hou [a], Chao Li [a], Heng Li [a]

[a] *China Lucky Film Group Corporation, Baoding, 071054, PR China*

[b] *University of Science and Technology of China, Hefei, 230026, PR China*

[*] Corresponding Authors.

Emails: zhuli12@mail.ustc.edu.cn (L. Zhu); lbli@ustc.edu.cn (L. Li)

1. Experimental section

1.1. Chemicals

Cerium nitrate (≥99.5%), glucose (≥98%), urea (≥99%), isopropanol (≥99.7%) and ethanol (99.7%) were commercially available and used without further purification. Octa(3-glycidyloxypropyl) polyhedral oligomeric silsesquioxane (GPOSS) was supplied by Hybrid Plastics, Inc; F127 (approximate molecular weight 12600) and triphenylsulfonium hexafluoroantimonate salts (TPS-HFAS, 50% purity in propylene carbonate) were purchased from Sigma-Aldrich; Polyethylene terephthalate (PET) was procured from Hefei Lucky Science & Technology Industry Co., Ltd. Deionized water with a resistivity of 18.25 MΩ·cm was used in all reactions.

1.2. Materials Characterization

Powder X-ray diffraction (XRD) patterns were acquired using a D/max-TTR III diffractometer with Cu Kα radiation (40 kV, 200 mA). Morphological characterization was carried out by field-emission scanning electron microscopy (FESEM, Hitachi S-4800) and transmission electron microscopy (TEM, JEM-2100). High-angle annular dark-field scanning transmission electron microscopy (HAADF-STEM) imaging and elemental mapping were performed using a spherical aberration-corrected FEI Titan G2 80-200 ChemiSTEM. Fourier-transform infrared (FT-IR) spectroscopy was conducted on an IRPrestige-21 spectrometer, covering the wavenumber range of 550-4000 cm^{-1}. X-ray photoelectron spectroscopy (XPS) measurements were obtained on an ESCALAB 250Xi spectrometer. UV-vis diffuse reflectance spectra (DRS) were recorded with a Hitachi U-3900 spectrophotometer. The Raman spectra were collected on a Bruker SENTERRA dispersive Raman microscope. The metal ions existing in the solution were analyzed by inductively coupled plasma mass spectrometry (ICP-MS) using a Thermo Fisher iCAP Pro. The specific surface area was analyzed by the Brunauer-Emmett-Teller method. The specific surface area was determined by the Brunauer-Emmett-Teller (BET) method via N_2 adsorption isotherms measured at 77 K using a Micromeritics ASAP 2020 surface area. The photoluminescence (PL) spectra were recorded on a Hitachi F-4500

fluorescence spectrophotometer and a Horiba Fluoromax Plus spectrometer. Thermogravimetric analysis (TGA) was performed on a Mettler Toledo TGA/DSC1/1100SF analyzer under a flowing nitrogen atmosphere, with the temperature ranging from 50 to 700 °C. The zeta potentials of CeO_2 NPs and CeO_2-B were measured using a Malvern Zetasizer Nano ZS90 spectrometer at room tempurature. Each sample was dispersed in deionized water at a concentration of 0.2 mg mL^{-1} and ultrasonicated for 30 min before measurement to ensure uniform dispersion.

Table S1 The haze date of pristine PET and CeO_2 NPs/PET.

Samples	Haze (%)
pristine PET	1.3
CeO_2 NPs/PET	1.7

Table S2 Comparison of UV-blocking performance of various material systems for polymer substrates.

Polymer substrate	UV blocking agents	UV cutoff (nm)	Visible transmitt-ance	Photostabili-ty	Other functional properties	Ref.
PET film	ZnO thin film	~370	53%	/	/	1
PET film	ZnTi-LDH/DL-1	~375	~60%	/	Enhanced mechanical property	2
PET film	ZnO-TiO_2 silane-Tinuvin	~350	90%	/	Enhanced hydrophobicity	3
PET film	SiO_2	~325	90%	/	Improved storage modulus	4
PET nonwovens	PVDF-SiO_2-CT	~355	/	/	/	5
PET fabrics	ZnO NPs	~350	/	/	Antibacterial	6
PET fabric	Cowpea proteins	~355	/	/	Enhanced wettability	7
Glass	F^- doped	350	80% (at	/	/	8

	CeO_2		500 nm)			
Glass	Nano-CeO_2	~350	~90%	36 h	Enhanced thermal stability	9
PMMA	CeO_2 NPs	~365	92%	/	/	10
PET film	CeO_2 NPs	~360	~86%	100 h, transmittance unchanged	Enhanced thermal stability and scratch resistance	**This work**

Table S3 The loading amount of CeO_2 in CeO_2 NPs/PET before and after immersed in deionized water for 10 days.

Samples	The loading amount of CeO_2 (wt%)
CeO_2 NPs/PET (before)	9.4
CeO_2 NPs/PET (after)	9.1

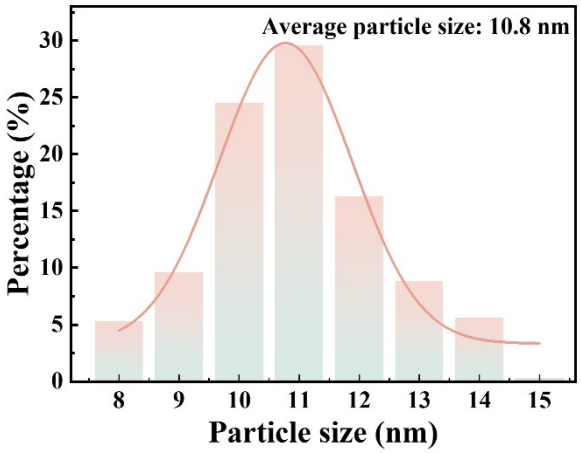

Fig. S1 Particle size distribution of CeO_2 NPs.

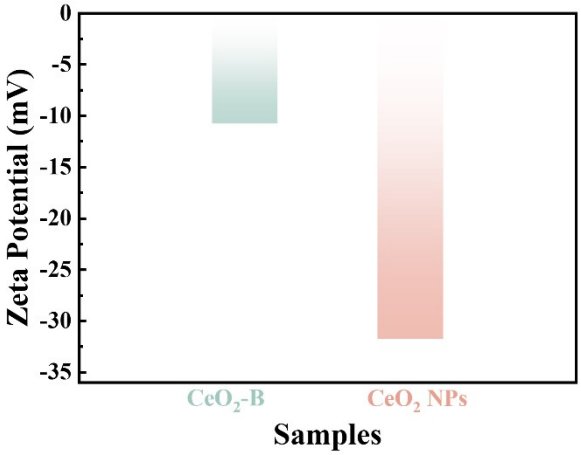

Fig. S2 Zeta potential of CeO_2 NPs and CeO_2-B.

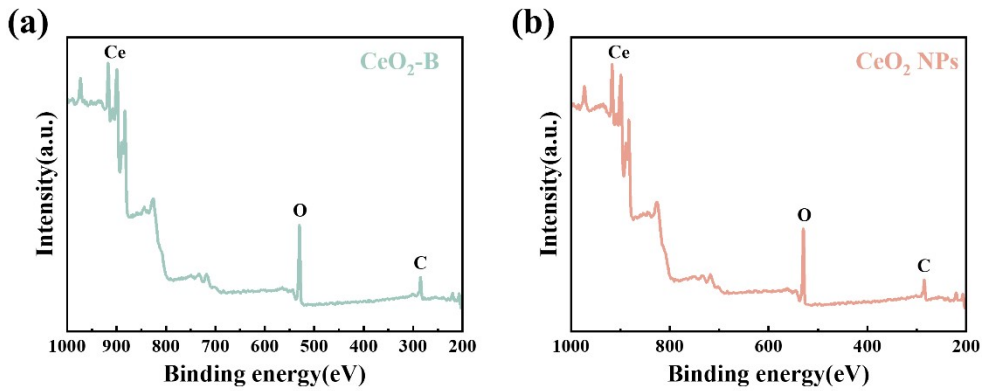

Fig. S3 XPS survey spectra of CeO_2 NPs and CeO_2-B.

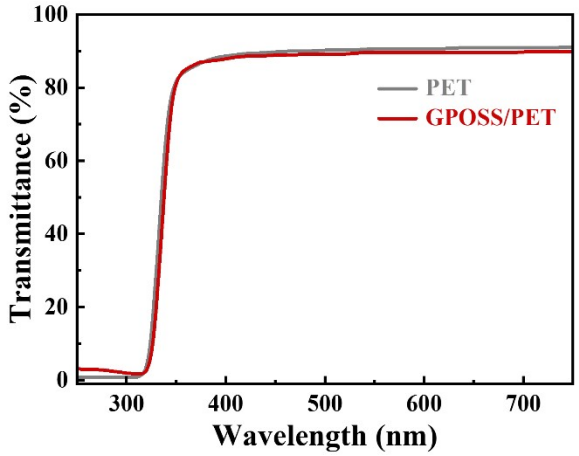

Fig. S4 UV-vis transmittance spectra of GPOSS on the PET films and pristine PET.

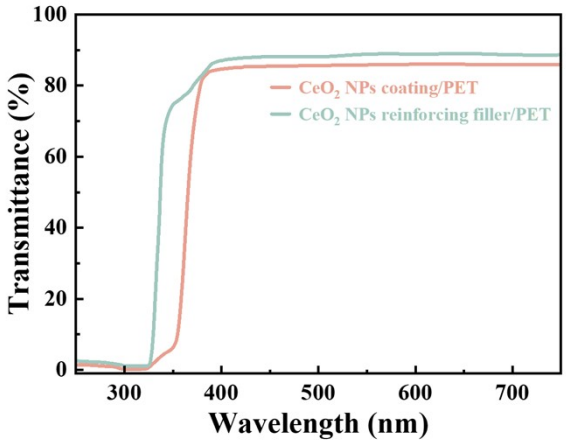

Fig. S5 UV-vis transmittance spectra of CeO_2 NPs coating and reinforcing filler (2000 ppm).

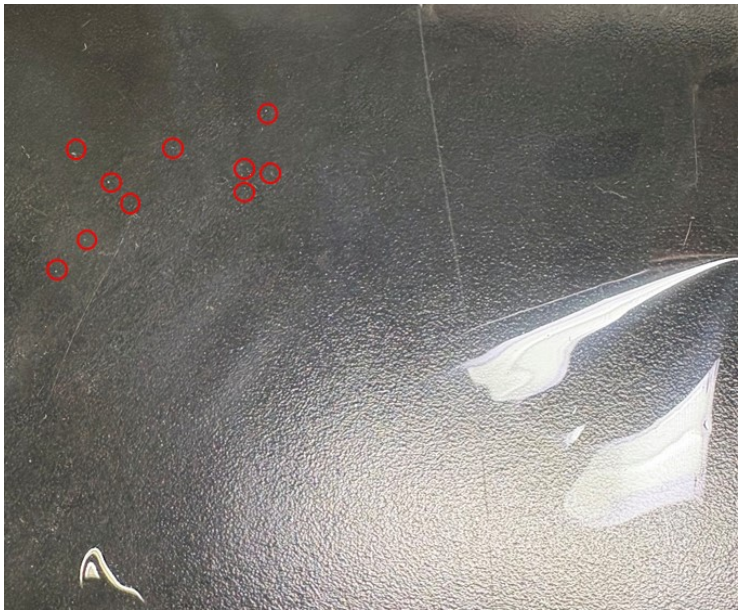

Fig. S6 Surface defects (pinholes and agglomerates) observed on the CeO_2 NPs reinforcing filler/PET film.

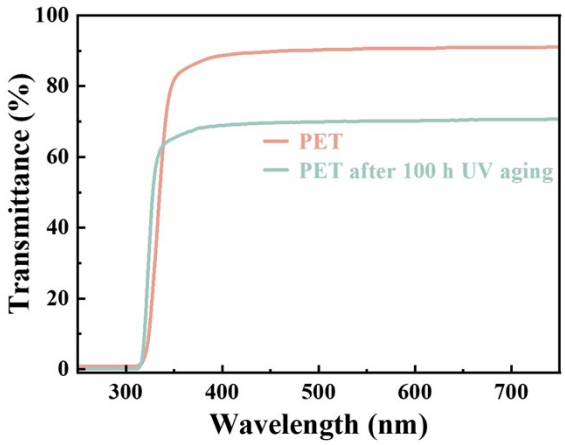

Fig. S7 UV-vis transmittance spectra of pristine PET film before and after 100 h UV aging.

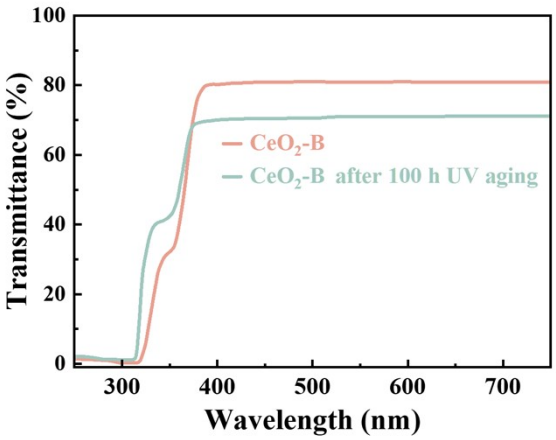

Fig. S8 UV-vis transmittance spectra of CeO_2-B coating on PET film before and after 100 h UV aging.

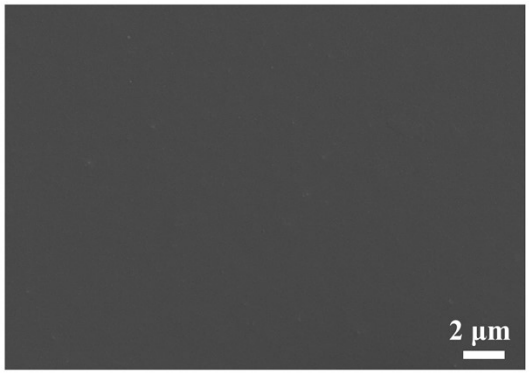

Fig. S9 SEM image of CeO_2 NPs/PET after immersed in deionized water for 10 days.

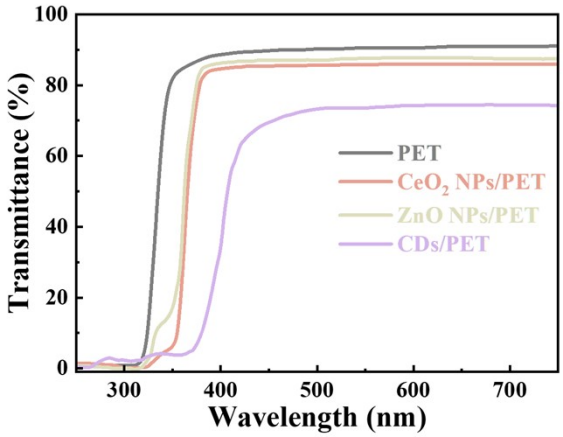

Fig. S10 UV-vis transmittance spectra of CeO_2 NPs, ZnO NPs and CDs coatings on PET films.

References

1 Q. Zheng, J. Huang, H. Li, L. Chen, Ceram. Int., 2019, 45, 3729-3734.

2 Y. Gao, H. Gui, J. Xu, R. Shen, L. Wei, X. Zhao, S. Zuo, J. Xu, X. Li, C. Yao, React. Funct. Polym., 2025, 212, 106249.

3 D. Yang, A.G. Ramu, D. Choi, Catalysts, 2022, 12, 1590.

4 T. Kang, L. Tang, J. Qu, Coatings, 2018, 8, 411.

5 N. Bouazizi, A. Abed, S. Giraud, A. El Achari, C. Campagne, M.N. Morshed, O. Thoumire, R. El Moznine, O. Cherkaoui, J. Vieillard, Phys. E, 2020, 118, 113905.

6 M.Z. Khan, H. Taghavian, J. Wiener, J. Militky, Y. Wang, B. Tomkova, M. Cernik, L. Dvorak, Surf. Interfaces, 2024, 55, 105336.

7 H. Sliman, X. Dong, T. Zhao, J. Colloid Interface Sci., 2020, 565, 360-367.

8 B. Bao, Y. Sun, X. Li, L. Li, Y. Yu, FlatChem, 2023, 39, 100494.

9 Y. Sun, G. Li, R. Zhong, RSC Adv., 2025, 15, 26266-26275.

10 M. Aklalouch, A. Calleja, X. Granados, S. Ricart, V. Boffa, F. Ricci, T. Puig, X. Obradors, Sol. Energy Mater. Sol. Cells, 2014, 120, 175-182.